

On the mechanism of oxidative electropolymerization and film formation for phenanthroline-containing complexes of ruthenium

Hai-Tao Zhang, Susan G. Yan, P. Subramanian, Lisa M. Skeens-Jones, Charlotte Stern, Joseph T. Hupp *

Department of Chemistry and Materials Research Center, Northwestern University, Evanston, IL 60208, USA

Received 27 June 1995; revised 22 February 1996

Abstract

New experiments involving electrochemistry, Auger spectroscopy and elemental analysis of films and film-forming compounds, as well as X-ray crystallography and electrochemistry of a key model compound, have been used to elucidate the linkage structure and probable mechanism of formation of oxidatively generated polymeric and copolymeric films of phenanthroline-containing complexes of ruthenium. Film formation evidently involves indirect electrochemical activation of coordinated 1,10-phenanthroline to nucleophilic attack by the non-coordinated pyridyl nitrogen of a dipyriddy ligand singly coordinated to a second metal center. The resulting linkage is comprised of a carbon/nitrogen bond with an excess positive charge residing on the nitrogen atom. Electrochemical oxidation of a complexed metal ion (typically Ru(II)) drives the polymerization by: (a) rendering the 4 site of phenanthroline significantly electrophilic, and (b) providing an oxidizing equivalent for eventual H atom elimination and pyridinium ion formation via an internal electron transfer sequence.

Keywords: Phenanthroline; Ruthenium; Electropolymerization; Film; Mechanism

1. Introduction

Some time ago we reported on the unexpected oxidative electropolymerization of ruthenium complexes of phenanthroline (phen) and either 4,4'-bipyridine (4,4'-bpy) or bis(4-pyridyl)ethylene (BPE). In dry acetonitrile solutions of $\text{Ru}(\text{phen})_2\text{L}_2^{2+}$, voltammetric cycling in the vicinity of the Ru(II/III) couple readily yielded bright orange films that were both electroactive and strongly adherent [1]. Experiments with several similar molecules pointed to the apparent need for both phen and singly-ligated, difunctional pyridine species L in the primary coordination sphere in order for polymerization to occur. Curiously, monomers featuring 2,2'-bipyridine (bpy) in place of phen did not electropolymerize detectably. (In a prior report, however, films were obtained via oxidative activation of $\text{Ru}(\text{bpy})\text{L}^{2+}$ (bpy = 2,2'-bipyridine; L = bis(4-pyridyl)ethyne) [2].) In any case, films generated in this way are of potential interest as redox conductors, as electrochromics [1,3], or in applications where systematic tuning of monomer–monomer linkage ligand L length is desired [4]. In this report we

describe electrochemical, analytical and X-ray crystallographic probes of the primary linkage structure and propose an electrochemical mechanism for film formation.

2. Experimental

2.1. Materials

Phen, 5-chloro-1,10-phenanthroline (5-Cl-phen), 5-methyl-1,10-phenanthroline (5-CH₃-phen) and 4,7-diphenyl-1,10-phenanthroline were purchased from GFS Chemicals. BPE, 4,4'-bpy, bis(4-pyridyl)ethane (BPA), 4,4'-trimethylenedipyridine (TMP), pyrazine (pz) and bpy were purchased from Aldrich Chemical Co. β,β' -bis(4-pyridyl)-1,4-diethylbenzene (BPEB) was prepared as previously described [4]. Ligand structures are shown in Fig. 1. Reagent grade acetonitrile and dichloromethane were purchased from Fisher and distilled from calcium hydride prior to use. Tetrabutylammonium perchlorate (TBAP) was purchased from GFS Chemicals; tetrabutylammonium hexafluorophosphate (TBAH) was purchased from Aldrich Chemical Co.

* Corresponding author.

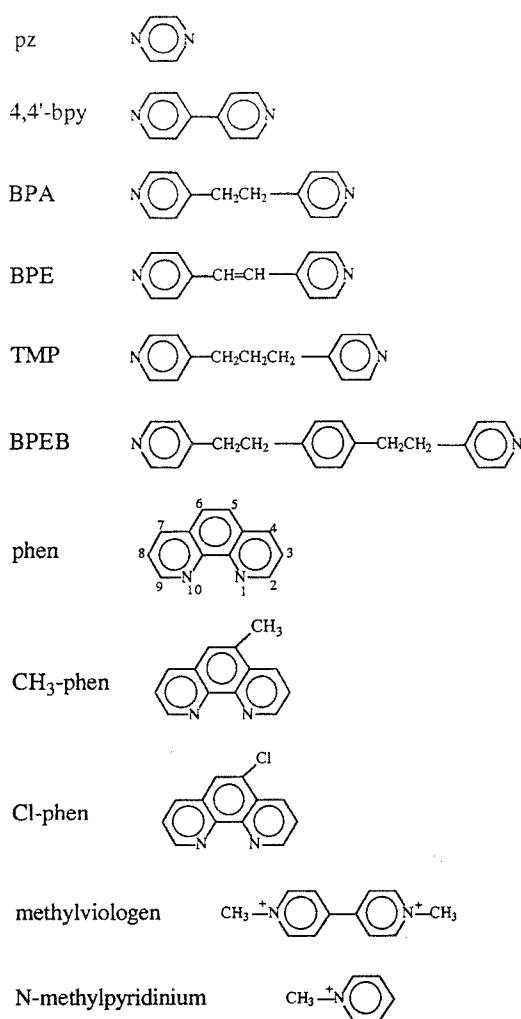


Fig. 1. Structures and abbreviations for ligands and related species.

Standard literature methods [1,3–8] were used to prepare and purify several compounds of the type $[\text{Ru}(\text{phen-X})_2\text{L}_2](\text{PF}_6)_2$, $[\text{Ru}(\text{bpy})_2\text{L}_2](\text{PF}_6)_2$, $[\text{Ru}(\text{phen-X})_3](\text{PF}_6)_2$, $[\text{Fe}(\text{phen-X})_3](\text{PF}_6)_2$, $[\text{Os}(\text{phen})_3](\text{PF}_6)_2$ and $[\text{Os}(\text{phen})_2\text{L}_2](\text{PF}_6)_2$ ($\text{X} = \text{H}$, 5-Cl, 5-CH₃, 5-Cl and/or 4,7-diphenyl; $\text{L} = \text{pz}$, 4,4'-bpy, BPE, BPA, TMP and/or BPEB). For new compounds, satisfactory elemental analyses (C, H, N) were obtained.

$[\text{Ru}(\text{phen})_2(\text{phen-4,4'-bpy})](\text{PF}_6)_3$ was prepared by first converting $\text{Ru}(\text{phen})_3^{2+}$ to $\text{Ru}(\text{phen})_3^{3+}$ (electrolysis in dry acetonitrile at +1.4 V with TBAH as supporting electrolyte). The oxidized solution (green) was added to an acetonitrile solution containing a several-fold excess of 4,4'-bipyridine. The solution turned orange essentially immediately, but was stirred for an additional hour. Solvent was removed by rotary evaporation. The residue was extracted several times with hot chloroform to remove unreacted TBAH. The crude product was purified by alumina column chromatography with 1:1 toluene + acetonitrile as eluent. Adequate separation of $\text{Ru}(\text{phen})_2(\text{phen-4,4'-bpy})_2^{3+}$ from $\text{Ru}(\text{phen})_3^{2+}$ was achieved only after three columns.

X-ray quality crystals of the purified sample were obtained after 7 days from an acetonitrile + toluene mixture held at 4°C.

2.2. Measurements

Cyclic voltammetry measurements were made using a Princeton Applied Research polarographic analyzer (Model 264A) and a Houston Instruments X-Y recorder (Model 2000). Electrochemical measurements were made in standard three compartment cells containing 0.1 M TBAP in acetonitrile (or dichloromethane for complexes containing BPEB) as solvent. The cells featured a 1 mm diameter platinum disk working electrode, a platinum wire counter electrode and a saturated (sodium chloride) calomel reference electrode (SSCE). Controlled potential coulometry (bulk electrolysis) was performed on a PAR 273 potentiostat using a platinum mesh working electrode.

Auger spectra for metallopolymeric films and related monomeric compounds (solvent evaporated residues) were obtained via electron excitation with a scanning Auger microprobe (Model 590A) manufactured by Physical Electronic Industries, Inc. For each specimen, four or five randomly selected spots were examined with the microprobe and spectra were collected in the derivative mode.

2.3. X-ray crystallography

A purple crystal of $\text{RuN}_8\text{C}_{49}\text{P}_3\text{F}_{18}\text{H}_{32}\text{O}$ was mounted on a glass fiber. Measurements were made on an Enraf-Nonius CAD-4 diffractometer with graphite monochromated Cu K α radiation. Cell constants and an orientation matrix for data collection, obtained from a least-squares refinement using the setting angles of 25 carefully centered reflections in the range $95.96^\circ < 2\theta < 97.70^\circ$, corresponded to a rhombohedral (hexagonal axes) cell with dimensions $a = 41.417(4) \text{ \AA}$, $c = 16.776(2) \text{ \AA}$ and $V = 24919(8) \text{ \AA}^3$. For $Z = 18$ and $FW = 1284.81$, the calculated density is 1.541 g cm^{-3} . Based on the systematic absences of hkl , $-h + k + l \neq 3n$, packing considerations, a statistical analysis of intensity distribution and the successful solution and refinement of the structure, the space group was determined to be $R\bar{3}(h)$ (No. 148).

The data were collected at a temperature of $-120 \pm 1^\circ\text{C}$ using the ω scan technique to a maximum 2θ value of 100.0° . Omega scans of several intense reflections, made prior to data collection, had an average width at half-height of 0.50° with a take-off angle of 2.8° . Scans of $(1.30 + 0.00\tan\theta)^\circ$ were made by scanning an additional 25% above and below the scan range. The counter aperture consisted of a variable horizontal slit with a width ranging from 2.0 to 2.5 mm and a vertical slit set to 2.0 mm. The diameter of the incident beam collimator was 0.7 mm and the crystal detector distance was 21 cm. For intense reflections an attenuator was automatically inserted in front of the detector.

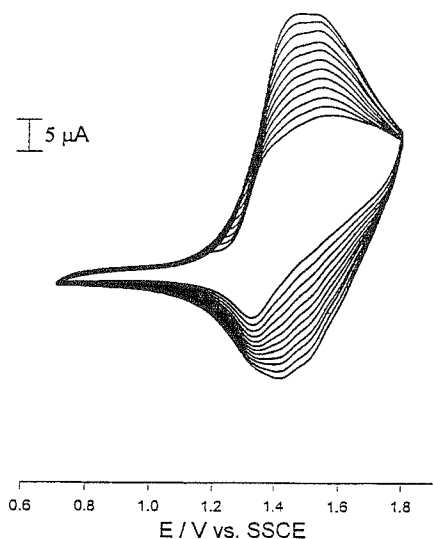


Fig. 2. Cyclic voltammetry of 1 mM $\text{Ru}(\text{phen})_2(4,4'\text{-bpy})_2^{2+}$ in acetonitrile as solvent; sweep rate 100 mV s^{-1} .

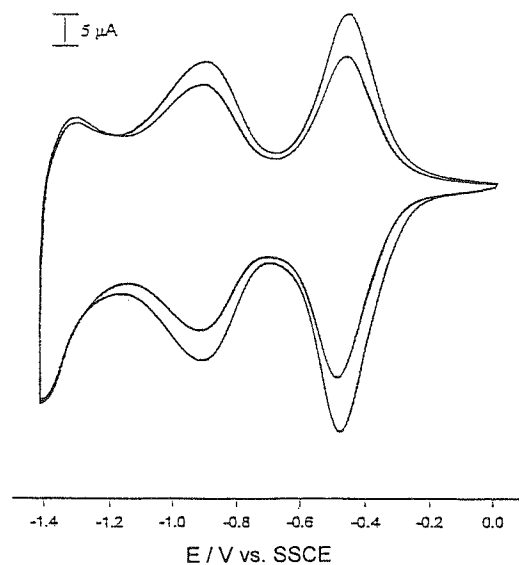


Fig. 3. Cyclic voltammetry (100 mV s^{-1} ; 0.1 M TBAP in acetonitrile) between 0 and -1.4 V for a poly- $\text{Ru}(\text{phen})_2(4,4'\text{-bpy})_2^{2+}$ film prepared in a similar fashion to that shown in Fig. 2.

Of the 11215 reflections collected, 6110 were unique ($R_f = 0.078$). The intensities of six reflections measured after every 180 min of X-ray exposure time remained constant throughout data collection, indicating crystal and electronic stability; therefore, no decay correction was applied. The linear absorption coefficient for Cu $K\alpha$ is 41.2 cm^{-1} . Azimuthal scans of several reflections indicated no need for an absorption correction. The data were corrected, however, for Lorentz and polarization effects.

The structure was solved by direct methods. The non-hydrogen atoms were refined either anisotropically or isotropically. The final cycle of full-matrix least-squares refinement was based on 3861 observed reflections ($I > 3.00\sigma(I)$) and 337 variable parameters and converged (largest parameter shift 8.99 times e.s.d.) with unweighted and weighted agreement factors of $R = 0.168$ and $R_w =$

0.210. The value of the goodness-of-fit parameter was 4.92. The level of refinement, therefore, is marginal for high precision bond-length determinations. It is clearly satisfactory, however, for establishing connectivity and approximate atom locations without ambiguity. All calculations were performed using the TEXSAN crystallographic software package (Molecular Structure Corp.).

3. Results and discussion

3.1. Electrochemical probes of linkage structure

Fig. 2 illustrates the cyclic voltammetric behavior of a representative monomer, $\text{Ru}(\text{phen})_2(4,4'\text{-bpy})_2^{2+}$. As in the

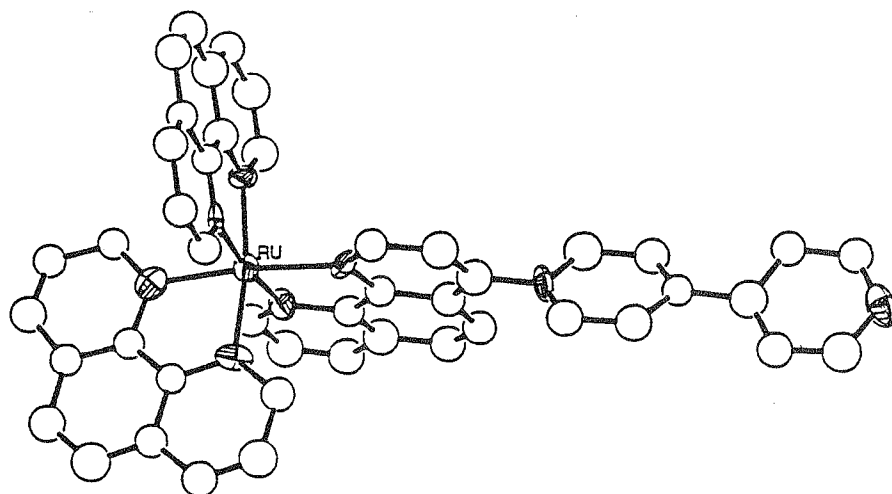


Fig. 4. ORTEP drawing of $\text{Ru}(\text{phen})_2(\text{phen-4,4'-bpy})_3^{3+}$.

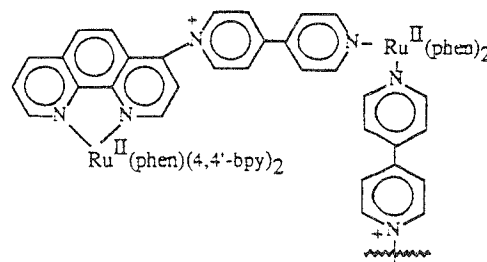
preliminary report [1], cycling in the vicinity of the Ru(II/III) couple (about 1.2 V) was accompanied by a progressive increase in current which is characteristic of formation and interfacial accumulation of redox active polymeric material. Removal of the electrode after several tens of cycles revealed an orange film that was retained during rinsing. Further voltammetric measurements after transfer of the electrode to a solution lacking the monomer showed that the film retained its electroactivity. Similar responses were obtained for phenanthroline ruthenium complexes containing BPE, BPA, TMP and BPEB. (A complex containing pz, however, failed to polymerize.)

Extension of the poly-Ru(phen)₂(4,4'-bpy)₂ⁿ⁺ voltammetry to negative potentials (Fig. 3) yielded an unusual response: reversible reduction peaks appeared at -0.46 and -0.88 V and persisted for several cycles after film formation. (Similar behavior is observed for films derived from Ru(phen)₂(BPE)₂²⁺.) Notably, these peaks are well positive of those expected for coordinated phen and 4,4'-bpy reduction. Interestingly, however, they resemble, at least superficially, the electrochemical behavior of methyl viologen, i.e. 1,1'-dimethyl-4,4'-bipyridinium (see Fig. 1). (Furthermore, as with methyl viologen, reduction of the film is accompanied by an intense blue color formation.) We surmised, therefore, that polymerization might be occurring via alkylation or arylation of the remote nitrogen of coordinated 4,4'-bipyridine to yield a linkage ligand featuring positive charges on or near both nitrogen atoms.

Similar experiments with films derived from either Ru(phen)₂(BPA)₂²⁺ or Ru(phen)₂(TMP)₂²⁺ yielded a single irreversible reduction ($E_{\text{peak}} \approx -0.8$ V) in the range +1 to -1 V. The reductive wave was observable, however, only on the first negative voltammetric scan. The response is similar, therefore, to that for the N-methylpyridinium cation (structure shown in Fig. 1), again suggesting that polymerization involves alkylation (or arylation) and positive charge generation at the remote nitrogen of the putative linkage ligand.

Returning to the voltammetric behavior in the oxidative region, three additional points are worth noting. First, the initial growth cycles are characterized by an enhanced Ru(II) oxidation current, but a diminished Ru(III) reduction current. This behavior is suggestive of a catalytic electrochemical/chemical (EC') reaction sequence. Secondly, the formal potential for the Ru(III/II) couple is significantly positively shifted following electropolymerization. Finally, multiple metal-based redox waves (overlapping) are evident in many film-based voltammograms, despite the existence of only a single wave in each of the monomer based voltammograms. We defer consideration of the first observation until a later section. The second and third observations, however, offer a basis for further speculation on the nature of the linkage chemistry. If remote pyridyl attachment occurs via nitrogen(pyridine)-carbon(phen) bond formation (see below), then the attached cation will exert an enormous inductive (electron

withdrawing) influence upon the phenanthroline-bound metal center. The inductive influence should be manifest as a positive shift in the Ru(III/II) potential. Additionally, if discrete film-based redox sites exist with one as well as two reacted phenanthroline ligands (or with doubly reacted phen ligands), then multiple metal-centered voltammetric peaks should be observed, with the most positive peaks corresponding to the most extensively reacted polymerization centers.



3.2. Micro Auger studies

If the linkage structure suggested above is correct, and if film formation leads to complete (or nearly complete) reaction of the available remote pyridyl functionalities, then the average charge per monomer unit should be 4+ in the Ru(II) form of the polymer. Similarly, the average number of singly charged counter anions should be four per metal center in the film environment. We have previously observed [5] that relative elemental compositions for films can be determined from ratios of micro Auger

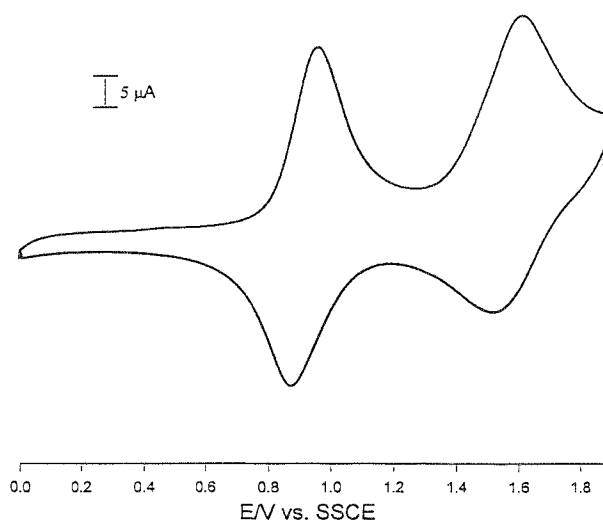


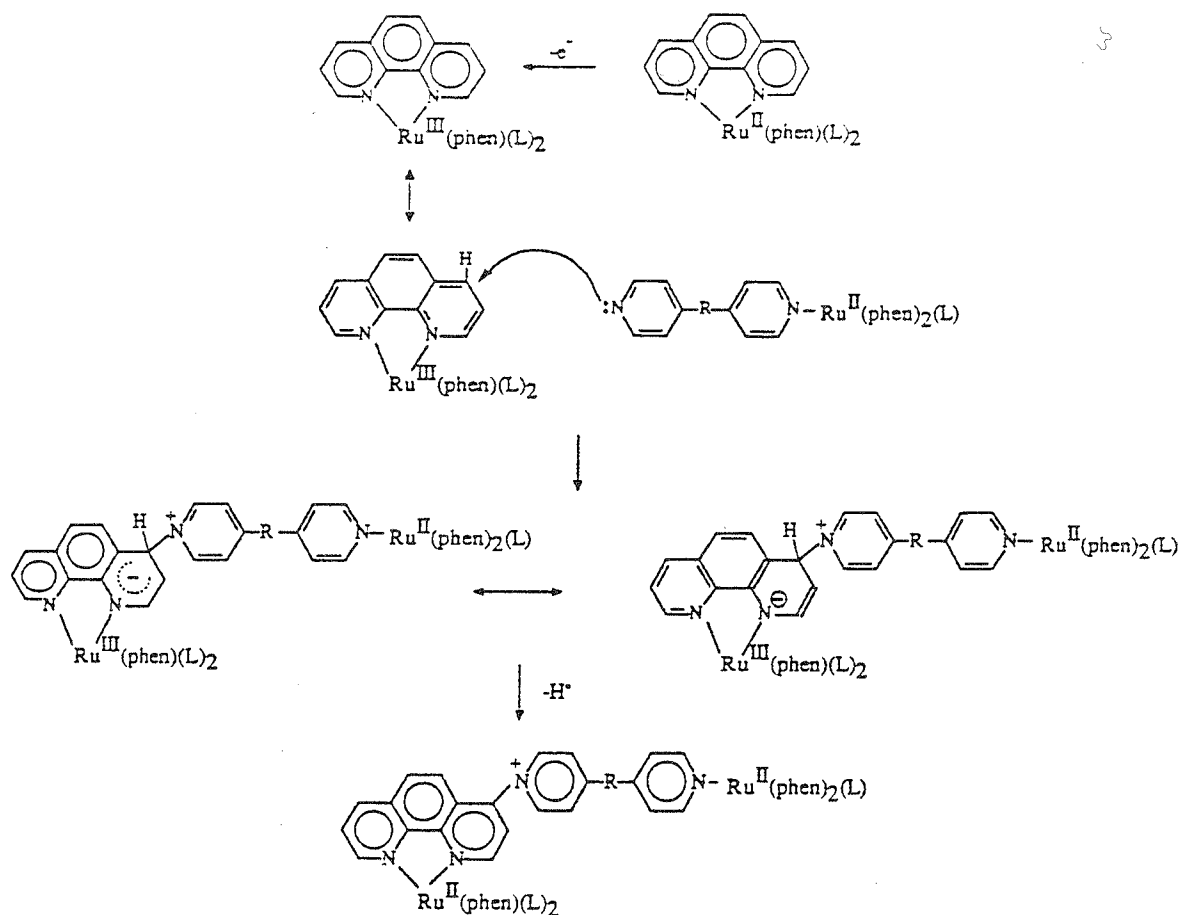
Fig. 5. Voltammetric response (100 mV s⁻¹; 0.1 M TBAP in acetonitrile) of a copolymeric film prepared by repetitive cycling (0 to 1.9 V) in a mixture containing 0.5 mM Ru(phen)₂(4,4'-bpy)₂²⁺ and 0.5 mM Os(phen)₂(4,4'-bpy)₂²⁺.

derivative peak intensities I . One of the easier intensity ratios to obtain experimentally is carbon to chlorine. For poly- $\text{Ru}(\text{phen})_2(4,4'\text{-bpy})_2^{n+}$ films grown in tetraethylammonium perchlorate solutions, we obtained $I_{\text{Cl}}:I_{\text{C}} = 0.41 \pm 0.03$. In part because absolute Auger electron ejection efficiencies differ for different elements, the intensity ratio alone is not meaningful. A calibration was provided, however, by measurements on the unreacted complex $[\text{Ru}(\text{phen})_2(4,4'\text{-bpy})_2](\text{ClO}_4)_2$, where the absolute chlorine to carbon ratio is known with certainty; these yielded $I_{\text{Cl}}:I_{\text{C}} = 0.19 \pm 0.03$. (**Caution:** Perchlorate salts of transition metal complexes are potentially explosive. They should be prepared and handled only in extremely small quantities.) Since the number of carbon atoms per metal center should be identical for the unreacted compound versus the metallopolymer (assuming that solvent (hydrocarbon) swelling of the polymer can be neglected), the estimated number of perchlorate ions per metal center is 4.3 ± 0.5 for the latter, consistent with the proposed linkage structure. Finally, the micro Auger results were semiquantitatively corroborated by conventional elemental analysis of films scraped from large area electrodes. The composition found was: C, 44.01; H, 3.30; N, 9.78; Cl, 10.00%. The composition expected for $\{[\text{Ru}(\text{phen})_2(4,4'\text{-bpy})_2](\text{ClO}_4)_4\}_n$

is: C, 45.01; H, 2.75; N, 9.56; Cl, 12.01%. For comparison, the composition expected for $\{[\text{Ru}(\text{phen})_2(4,4'\text{-bpy})_2](\text{ClO}_4)_2\}_n$ would be: C, 54.32; H, 3.31; N, 11.51; Cl, 7.29%.

3.3. X-ray crystallographic studies

In principle, the most rigorous method of establishing chemical structures is single crystal X-ray diffraction. Unfortunately, metallopolymeric films are amorphous and therefore unsuitable for high quality diffraction studies. Nevertheless, we reasoned that the crucial linkage structure could be characterized by examining a monomeric analog prepared in the same fashion as the polymeric species. As indicated above, the monomer was obtained by combining electrogenerated $\text{Ru}(\text{phen})_3^{3+}$ with 4,4'-bipyridine. The isolated product, $[\text{Ru}(\text{phen})_2(\text{phen-4,4'-bpy})](\text{ClO}_4)_3$, yielded (via X-ray structural analysis) the structure shown in Fig. 4. For our purposes, the most important findings are: (a) the formation of a single bond between one of the two available bipyridyl nitrogens and a carbon at the 4 position of phenanthroline; (b) retention of ring planarity, indicating retention of sp^2 hybridization at C4 and elimination, therefore, of a H atom, and (c) the presence of three



Scheme 1.

counter ions (not shown). Visible region absorption measurements show that ruthenium exists in oxidation state II. The excess positive charge, therefore, almost certainly resides at the bipyridyl nitrogen involved in linkage formation. Electrochemical studies of the X-ray characterized compound revealed an irreversible reduction at ca. -0.54 V (sweep rate 200 mV s^{-1}), which can now be unambiguously assigned to monoarylated bipyridinium reduction. Further studies revealed that the compound could be oxidatively electropolymerized, and that polymerization is accompanied by film formation. Given the monomer structure (i.e. only one unreacted nitrogen) these particular films must be comprised, however, of “linear” chain polymers rather than cross-linked polymers (the likely form for $\text{Ru}(\text{phen})_2\text{L}_2^{2+}$ -derived materials).

3.4. Electrochemical mechanistic studies

With the nature of the linkage structure established, the key remaining question is the mechanism of linkage formation. The available observations are that: (1) polymerization occurs only after metal oxidation, likely via an EC' or similar mechanism; and (2) polymerization occurs with phenanthroline, but not with 2,2'-bipyridine. We sought to supplement these by examining several additional monomers and mixtures of monomers. Among the additional studies was one involving replacement of ruthenium by osmium in $\text{M}(\text{phen})_2(4,4'\text{-bpy})_2^{2+}$. The consequences were the expected decrease in the $\text{M}(\text{III}/\text{II})$ formal potential (to ca. 0.85 V), but the unexpected loss of nearly all propensity towards electropolymerization. (For example, fewer than five molecular monolayer equivalents of film material were generated in 30 min of voltammetric cycling.) Interestingly, however, the osmium compound readily copolymerized with $\text{Ru}(\text{phen})_2(4,4'\text{-bpy})_2^{2+}$ (Fig. 5).

The Os/Ru comparison implies that oxidative activation (at least for single monomer solutions) requires a relatively positive formal potential. To test this idea further, metal centered formal potentials were adjusted in a more subtle fashion. Fig. 6 compares electropolymerization experiments for monomers of the type $\text{Ru}(\text{X-phen})_2(\text{BPA})_2^{2+}$, where $\text{X} = \text{CH}_3$, H or Cl. From the figure, the observed reactivity order is $\text{Cl} > \text{H} > \text{CH}_3$, in agreement with the ordering of $\text{Ru}(\text{III}/\text{II})$ potentials.

With the additional observations, we propose that polymerization is initiated by nucleophilic attack by a pyridyl nitrogen at the 4 (or 7) position of phenanthroline (Scheme 1; note that non-reactive hydrogens are omitted from the diagram). Importantly, the attack site is activated (i.e. rendered more electrophilic) by coordinated metal oxidation. Similar oxidation-based activation of phen complexes has been reported by Kochi and coworker in their studies of alkyl radical addition reactions [9,10]. A precedent also exists from a study by Stanbury and coworkers on the oxidative activation of $\text{Ru}(\text{NH}_3)_4(\text{phen})^{2+}$ to addition of

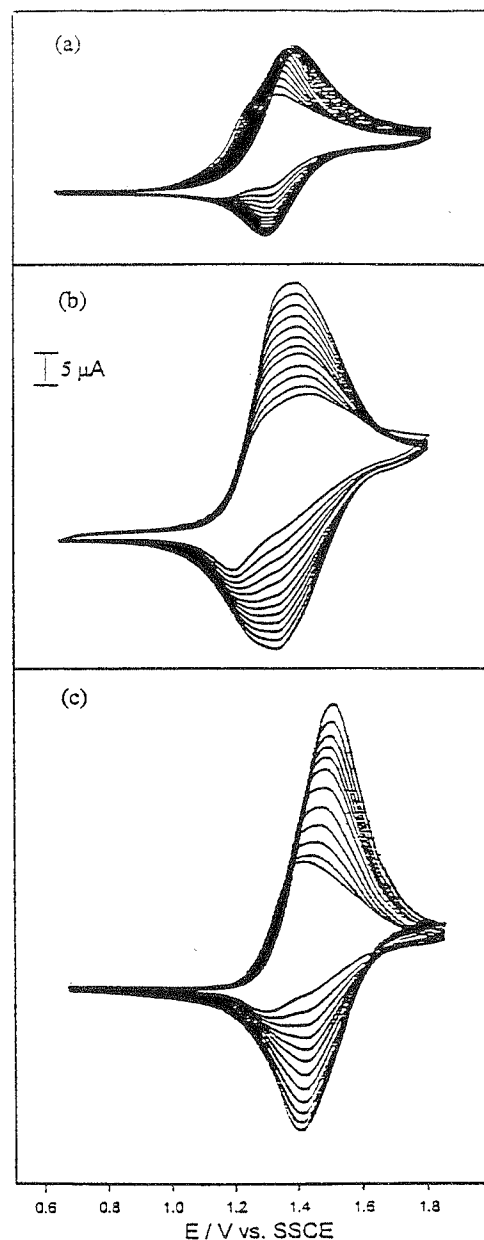


Fig. 6. Cyclic voltammetry (100 mV s^{-1} ; first 12 cycles) and polymer film growth for $\text{Ru}(\text{X-phen})_2(\text{BPA})_2^{2+}$ species (0.5 mM) in acetonitrile as solvent: (a) $\text{X} = \text{CH}_3$; (b) $\text{X} = \text{H}$; (c) $\text{X} = \text{Cl}$.

SO_3^{2-} , probably via a mechanism involving intermediate radical generation [11]. Interestingly, in both studies the active site was the 4 position of phenanthroline. Furthermore, in both studies substituent addition was accompanied by metal reduction and H (or H^+) elimination. In any case, Kochi and coworker have pointed out that if C–H bond cleavage is coupled to a rate determining internal electron transfer (effectively ligand to metal), then substituent addition will become more rapid (and more efficient) when the $\text{M}(\text{III}/\text{II})$ formal potential is made more positive. We suggest that a similar rate determining internal electron transfer step exists in the nucleophilic addi-

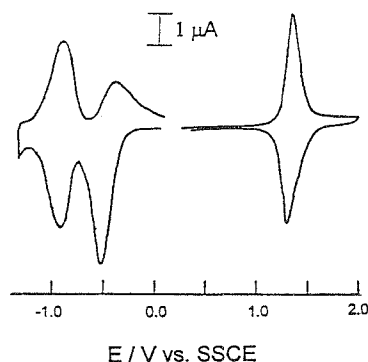


Fig. 7. Voltammetric response (100 mV s^{-1} ; 0.1 M TBAP in acetonitrile) of a copolymeric film prepared by repetitive cycling in a mixture containing 2 mM $\text{Ru}(\text{phen})_3^{2+}$ and 2 mM $\text{Ru}(\text{bpy})_2(4,4'\text{-bpy})_2^{2+}$.

tion/polymerization reaction (Scheme 1), as shown by the almost complete inhibition of electropolymerization upon replacement of $\text{Ru}(\text{III})$ by the less readily reduced $\text{Os}(\text{III})$ center. (In principle, C–H bond cleavage could also occur heterolytically, i.e. via proton rather than H atom elimination. This would require participation of a second ruthenium center as an outer sphere source of an additional oxidizing equivalent. Our electrochemical and structural findings are consistent with either elimination mechanism.) Note that an internal ET process would also account for the apparent EC' type behavior in Fig. 1 and for the reduction of $\text{Ru}(\text{phen})_3^{3+}$ by 4,4'-bipyridine in the monomer model complex synthetic studies. Finally, the internal electron transfer scheme (or a close variant) would also account for the phen substituent-based modulation of reactivity illustrated in Fig. 6. Alternatively (or additionally) the reactivity pattern in Fig. 6 might be ascribed simply to inductive tuning of the electrophilic character of the C4 site on phenanthroline.

In view of the proposed mechanism, one additional series of experiments was attempted. The objective was to determine whether films could be grown from pairs of monomers that were separately non-polymerizable (or barely polymerizable), but together contained the requisite dipyrityl and phen ligands. Fig. 7 shows, for example, that electroactive films can be prepared oxidatively from solutions containing both $\text{Ru}(\text{phen})_3^{2+}$ and $\text{Ru}(\text{bpy})_2(4,4'\text{-bpy})_2^{2+}$. Films are also readily obtained from mixtures of $\text{Ru}(\text{Cl-phen})_3^{2+}$ and $\text{Ru}(\text{bpy})_2(4,4'\text{-bpy})_2^{2+}$ (where again neither component appreciably oxidatively electropolymerizes separately). Films are not obtained, however, from mixtures of $\text{Ru}(\text{bpy})_2(4,4'\text{-bpy})_2^{2+}$ and either $\text{Fe}(\text{phen})_3^{2+}$ ($E_f = 1.10 \text{ V}$) or $\text{Os}(\text{phen})_3^{2+}$ ($E_f = 0.82 \text{ V}$), presumably because the 3+ forms of the phen complexes lack the necessary driving force for rapid H atom elimination. $\text{Fe}(\text{Cl-phen})_3^{2+}$ ($E_f = +1.17 \text{ V}$), however, does copolymerize with $\text{Ru}(\text{bpy})_2(4,4'\text{-bpy})_2^{2+}$, albeit relatively slowly. Finally, we have found that copolymer film growth

($\text{Ru}(\text{bpy})_2(4,4'\text{-bpy})_2^{2+} + \text{Ru}(\text{phen-R}_2)_3$) can be inhibited (but not completely prevented) by chemically blocking the reactive 4 and 7 sites of phen with phenyl substituents (i.e. by replacing the reactive C–H bond with a less reactive (and less accessible) C–C bond). Presumably, the residual reactivity is associated with substitution at an alternative site [9].

4. Conclusions

Oxidative electropolymerization of $\text{M}(\text{phen})_2\text{L}_2^{2+}$ species entails the formation of arylated pyridinium linkages. The probable mechanism of linkage formation is nucleophilic attack by a free pyridyl nitrogen at the 4 position of coordinated phenanthroline, followed by reduction of the metal center (by internal charge transfer) and elimination of a H atom. The metal reduction step is evidently rate determining. The rate of electropolymerization, therefore, is strongly dependent upon the $\text{M}(\text{III}/\text{II})$ formal potential, with the fastest polymerization reactions occurring for the monomers displaying the most positive potentials.

Acknowledgements

We thank Professor James Ibers for providing access to equipment for X-ray data collection. We thank the Office of Naval Research and the NSF Materials Research Center at Northwestern (DMR-9120521) for support of our work. JTH also gratefully acknowledges unrestricted support from the Dreyfus Foundation (Teacher–Scholar Award, 1991–1996).

References

- [1] O.R. Fussa-Rydel and J.T. Hupp, *J. Electroanal. Chem.*, 251 (1988) 147.
- [2] J.M. Calvert, D.L. Peebles and R.J. Nowak, *Inorg. Chem.*, 24 (1985) 3111.
- [3] H.T. Zhang, P. Subramanian, O. Fussa-Rydel, J.C. Bebel and J.T. Hupp, *Solar Mater. Solar Cells*, 25 (1982) 315.
- [4] S.G. Yan and J.T. Hupp, *J. Electroanal. Chem.*, 397 (1995) 119.
- [5] O.R. Fussa-Rydel, H.T. Zhang, J.T. Hupp and C.R. Leidner, *Inorg. Chem.*, 28 (1989) 1533.
- [6] J.M. Calvert, R.H. Schmehl, B.P. Sullivan, J.S. Facci, T.J. Meyer and R.W. Murray, *Inorg. Chem.*, 22 (1983) 2151.
- [7] D.A. Buckingham, F.P. Dwyer, H.A. Goodwin and A.M. Sargeson, *Aust. J. Chem.*, 17 (1964) 325.
- [8] F.H. Burstall and R.S. Nyholm, *J. Chem. Soc.*, (1952) 3570.
- [9] K.L. Rollick and J.K. Kochi, *J. Org. Chem.*, 47 (1982) 435.
- [10] K.L. Rollick and J.K. Kochi, *Organometallics*, 1 (1982) 725.
- [11] R. Sarala, M.A. Islam, S.B. Rabin and D.M. Stanbury, *Inorg. Chem.*, 29 (1990) 1133.